The Astrophysical Journal Letters, 727:L44 (4pp), 2011 February 1 doi:10.1088/2041-8205/727/2/L44

A SHORT-PERIOD CENSOR OF SUB-JUPITER MASS EXOPLANETS WITH LOW DENSITY

Gy. M. Szabó[1,3] and L. L. Kiss[1,2]
[1] Konkoly Observatory of the Hungarian Academy of Sciences, P.O. Box 67, H-1525 Budapest, Hungary
[2] Sydney Institute for Astronomy, School of Physics A28, University of Sydney, NSW 2006, Australia
Received 2010 November 8; accepted 2010 December 20; published 2011 January 12

ABSTRACT

Despite the existence of many short-period hot Jupiters, there is not one hot Neptune with an orbital period less than 2.5 days. Here, we discuss a cluster analysis of the currently known 106 transiting exoplanets to investigate a possible explanation for this observation. We find two distinct clusters in the mass–density space, one with hot Jupiters with a wide range of orbital periods (0.8–114 days) and a narrow range of planet radii ($1.2 \pm 0.2\ R_J$) and another one with a mixture of super-Earths, hot Neptunes, and hot Jupiters, exhibiting a surprisingly narrow period distribution (3.7 ± 0.8 days). These two clusters follow strikingly different distributions in the period–radius parameter plane. The branch of sub-Jupiter mass exoplanets is censored by the orbital period at the large-radius end: no planets with mass between 0.02 and 0.8 M_J or with radius between 0.25 and 1.0 R_J are known with $P_{\rm orb} < 2.5$ days. This clustering is not predicted by current theories of planet formation and evolution, which we also review briefly.

Key words: planets and satellites: general

Online-only material: color figures

1. INTRODUCTION

In circumstellar disks with ongoing planet formation, protoplanets accrete the gaseous matter of the disk. The initial mass spectrum of planets will depend on the orbital distances via the thermal and tidal effects of the star. Initial mass functions cover a wide range of masses, exhibit a bimodal or multimodal distribution, peaking near the mass of Neptune and Jupiter. Both peaks move to larger masses with increasing orbital periods. A key feature of the population in the 1–16 day orbital period range is that hot Neptunes always significantly outnumber hot Jupiters (Broeg 2006), which has been confirmed by observations recently in the 3–100 day period range (Howard et al. 2010). The observational confirmation of the mass spectrum is a direct tracer of the physical processes of planet formation in the nebular phase and the further evolution.

As of the writing of this paper, 106 transiting exoplanets have been published for which precise masses, radii, and orbital periods are known (Schneider 2010). This number of transiting planets is sufficient to perform statistical tests. The most important planet parameters are mass and radius, being the prime tracer of the interior structure (e.g., Guillot 2005; Fortney et al. 2007; Chabrier et al. 2009). Because there are obvious selection effects in the currently known exoplanet sample, tests should either concentrate on unbiased parameters, such as orbital periods, or on the combination of biased parameters, such as masses versus radii.

In this Letter, we demonstrate that exoplanets in the mass–density space fall into two clusters which follow very different period–radius distributions. Comparison of these samples shows that the observed lack of hot Neptunes and hot sub-Jupiters is censored at <2.5 day period range, while hot Jupiters do not suffer a similar censor. We address several candidate scenarios that may explain the observed period–mass distributions.

[3] Hungarian Eötvös Fellow at the University of Texas at Austin.

2. CLUSTER ANALYSIS OF THE DATA

Color-coding the points in one distribution and then plotting another diagram with the specified colors is a powerful technique to find clusters heuristically (see, e.g., a nice example in Ivezić et al. 2002 for solar system asteroids). Existence and structure of the suspected clusters can further be investigated by statistical tools. For such an analysis, we collected data from the Interactive Extrasolar Planet Catalog (Schneider 2010 and references therein). We included mass, size, average density, period, semimajor axis and inclination, and stellar parameters in our analysis. Drawing a few color-coded plots with a trial-and-error strategy, we have found that color-coding from the mass–density space distinguishes two different sequences in the period–radius space. Based on this finding, we propose a discrimination diagram in the mass–density space, separating two subclasses of exoplanets, hereafter D_1 (objects with lower mass) and D_2 (objects with larger mass, right to the borderline).

In panel (a) of Figure 1, we plot all the involved transiters in the mass–density space. With purpose of illustration, the 500 Myr isochrone of exoplanets at 0.045 AU distance to a solar analog is indicated (Fortney et al. 2007). The models contain 50% silicate and 50% water core with various initial masses indicated by the labels, and total mass indicated in the abscissa.

The border between the two clusters (panel (b) of Figure 1) was determined by maximizing the Mahalanobis distance (Mahalanobis 1936) of the two distributions in the period–radius space (see details in the Appendix). Mahalanobis distance has been successfully used in clustering data with severe correlations (De Maesschalck et al. 2000). The borderline between the two clusters has the equations of $\log(\rho) = 0.12513 \log(M - 0.30779)^{-0.83645}$, cluster D_1 is to the left (open symbols in panel (b) of Figure 1), while D_2 is to the right.

This classification can in part be assigned to objects discriminated by mass. D_1 exoplanets contain super-Earths (Valencia et al. 2007; Adams et al. 2008), hot Neptunes, and low-mass, low-density hot Jupiters. Hot Jupiters exceeding the mass or the density of Jupiter are assorted in D_2. For the sake of a suggestive

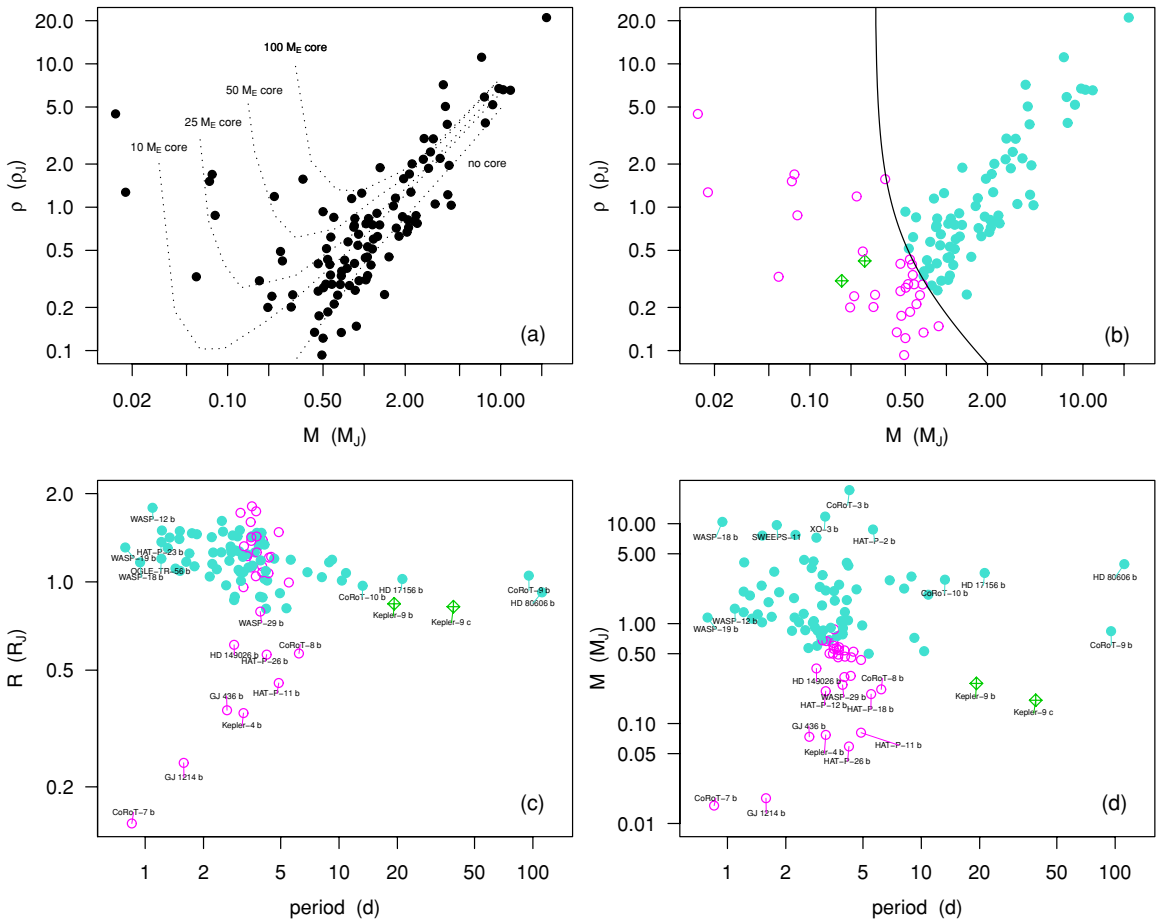

Figure 1. (a) The mass–density diagram of the currently known transiting exoplanets. Four planetary models with various core masses and one other without a core are plotted with illustrative purposes. (b) The proposed clustering in the mass–density space. Open and filled dots (magenta and blue online) distinguish the two clusters. Two planets, Kepler 9b and c are plotted with diamonds. (c) Clusters form two apparent sequences in the period–radius space. Note the lack of D_1 exoplanets with period < 2.2 days. (d) The distribution of the cluster members in the period–mass space.

(A color version of this figure is available in the online journal.)

distinction, D_1 may be referred as sub-Jupiters though cluster membership slightly depend on density, too. For example, a planet with 0.6 Jupiter mass will be D_2 if its density is around that of Jupiter and will be D_1 if the density is significantly lower.

3. RESULTS

The defined clusters (panel (b) of Figure 1) are well separated in the period–radius and period–mass parameter planes (panels (c) and (d)). D_2 cluster members cover a period range of more than two orders of magnitude, beginning from 0.7 days. The radius of D_2 members is indicatively 1–2 times that of Jupiter, slightly decreasing with orbital period (panel (c) of Figure 1, solid dots). The dependence of radius on period is due to the sensitivity of planet atmospheres to stellar irradiation (Fortney et al. 2007).

Transiters in D_1 cluster exhibit a narrow period distribution: 85% of them lie in the 2.5–5 day range. The branch of massive D_1 members overlaps with D_2 cluster members at the large-radius end in the period–radius space. All D_1 cluster members have periods >2.88 days in the $R > 0.5\ R_J$ size range, while there are 33 hot Jupiters in the 0.79–2.88 day orbital period range. Because these planets have similar radius and only their density differs, we conclude that the density is a major parameter in relation to the period censor.

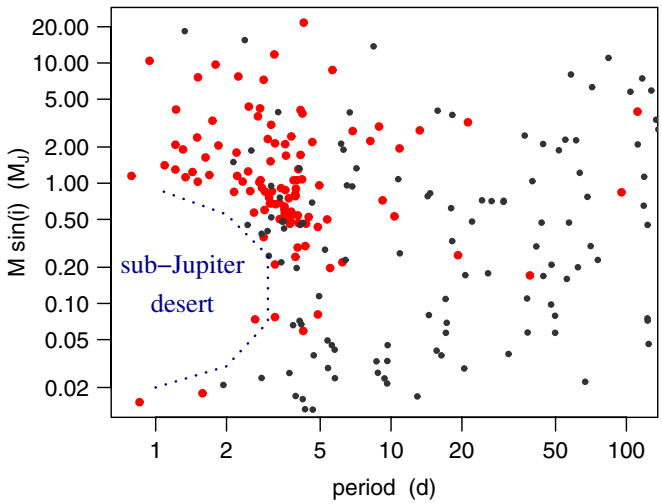

Figure 2. Period–minimum mass diagram of the currently known exoplanets. Large (red) dots: transiters; small (gray) dots: non-transiting planets. The axis ranges fit panel (d) of Figure 1.

(A color version of this figure is available in the online journal.)

Kepler 9b and c (Holman et al. 2010) are two important outliers with orbital periods of 19.2 and 38.9 days. However, these planets exhibit prominent variation of the period together with

transit timing variations as signatures of gravitational interaction of two planets near the 2:1 orbital resonance (Holman et al. 2010). Because of this known instability, they are designated with diamond symbols (green online).

In the lower two panels of Figure 1, a period desert of D_1 exoplanets is apparent, outlined by planets CoRoT-7b, GJ 1214 b, GJ 436 b, and HD149026 b. This means that no sub-Jupiters have orbital period less than 2.5 days, except the super-Earths. In the followings we estimate the probability of a low-period desert in the D_1 sample to occur by chance. There are two of 31 (6.5%) D_1 exoplanets with a period less than 2.5 days. The upper boundary of the period range of D_1 exoplanets is 7 days. We compare the period distribution of D_1 exoplanets to hot Jupiters which have period less than 2.5 days. There are 64 transiting hot Jupiters within this period range, and 24 of them (38%) have a period less than 2.5 days.

The two-sided Fisher's exact test (Fisher 1925; Douglas 1976) is a statistical test used to determine if there are nonrandom associations between two categorical variables. Testing the above contingencies, the asymmetric distribution is confirmed at the 99% confidence level, which is an evidence for the presence of a low-period desert in the data. The period censor does not affect large density hot Jupiters, which are evidently seen at the large-radius end of the D_1 distribution, where it overlaps with D_2s. The censor may be density selective, and this would be the primary cause of the "hole" in the period–radius distribution.

The period–mass diagram can be completed with non-transiting exoplanets. In this case the minimum mass, $M \sin i$, is known, and mass information is ambiguous to some extent. This is not a serious problem because the sub-Jupiter desert has an extension of 1.5 orders of magnitude in mass, and the hole in the period–mass distribution will remain recognizable. In Figure 2 we plot minimum mass versus period, using different symbols for transiters and non-transiting planets. Because of the strategy of radial velocity surveys, the period distribution of non-transiting planets is Nyquist-limited at around $P \approx 2$ day frequency, and there they exhibit not much overlap with the sub-Jupiter desert. However, there are nine non-transiting planets with orbital periods shorter than 3 days, falling around the long-period edge of the desert, but none coinciding with the desert itself. The lack of sub-Jupiters with semimajor axes less than 0.03 AU, or at least an anticorrelation between mass and semimajor axis, was suggested by previous authors (e.g., Winn et al. 2011). It has to be noted that the "hole" is more apparent in the period–radius distribution that we plot in this Letter. Moreover, we concluded that there are important sub-structures in the distribution: nearly zero or slightly positive correlation exists between the period and the radius of D_1 exoplanets, and a very slight anticorrelation exists for hot Jupiters.

4. DISCUSSION

In contradiction with the current models of planet formation nearby a star (e.g., Broeg 2009), we found that sub-Jupiter exoplanets (more exactly: the D_1 cluster members in the mass–density parameter space) exhibit a desert for $P_{\rm orb} <$ 2.5 day periods. The observed distribution is inconsistent with models assuming that most planets are born near or beyond the snow-line and then migrate inward (Ida & Lin 2008; Mordasini et al. 2009). These models lead to a super-Earth desert predicting a paucity of planets in the mass range of 1–30 $M_{\rm Earth}$ and orbiting inside 1 AU. Instead, our analysis showed that there are many sub-Jupiters between 3 and 5 day orbital period, which confirms the conclusion of Howard et al. (2010), telling that the current population synthesis models are inadequate to explain the distribution of low-mass planets.

Discussing possible modifications of planet formation models lies outside of the scope of this work, but here we suggest some possible hypotheses to account for.

1. Hot Neptunes may evaporate rapidly in the close vicinity of the star. Highly exposed planets with less potential energy evaporate more rapidly (Lecavelier des Etangs 2007), which can be a candidate explanation for the period censor. An argument for this procedure is the dependence of D_1–D_2 clustering on the density: planets with loose atmospheres are classified as D_1 in the mass range of 0.5–1 M_J. Indeed, these are the planets that exhibit the period censor.
   However, the presence of short-period super-Earths raises questions in regards to the evaporation framework. The internal energy of their atmosphere, if there is any, is evidently low and they should evaporate more rapidly than Neptunes. In the contrary, the hot super-Earth GJ 1214 is considered to have a thick atmosphere (Rogers & Seager 2010). A possible explanation could be that the incident UV flux is low around the host M dwarf star and the atmosphere can survive.
2. As sufficient explanation for the low-period desert, one could assume that hot Neptunes spiral in or migrate outward in a short timescale, while hot Jupiters do not. An argument against the selective in-spiraling of hot Neptunes is found by Armitage (2007), concluding that the mass function is not affected significantly by migration. Since many hot Jupiters with orbital periods of 0.7–2.5 days survived type II/III migration, it may be difficult to explain why hot Neptunes did not. Tidal disruption cannot explain the censor either, because hot super-Earths with 1 day orbital periods are still stable against tidal disruption (Schlaufman et al. 2010). Hot Neptunes can migrate outward (Martin et al. 2007), a process that could also have evacuated the sub-Jupiter desert. However, outward migration requires a massive inner planet (Martin et al. 2007), which is lacking in the case of the known hot Neptunes.
3. Based on their completely different distributions in the period–mass diagrams, one could assume that D_1 and D_2 planets differ in the amount and strength of planet–planet perturbation. However, this idea is generally challenged by the distribution of eccentricities and stellar obliquity. Both D_1 and D_2 cluster exoplanets share similar eccentricity properties, probably reflecting similar perturbation history. To check this, we applied a Kolmogorov–Smirnov test to the eccentricities of D_1 and D_2 members, resulting in a $p = 0.55$ value, suggesting that the eccentricities are very similarly distributed. Stellar obliquities follow a similar distribution in D_1 and D_2, too. There are nine systems with large stellar obliquity known among D_2 exoplanets and two are known in the D_1 cluster. Confirmed by a Fischer's Exact Test, there is no significant difference in the occurrence of large obliquity.
4. The observed long-period edge of the sub-Jupiter desert fits the type I migration model predictions of Masset et al. (2006) with disk torques accounted. Near the disk cavity, a density radial jump forms in the protoplanetary nebula. In the theory of Masset et al. (2006), low-mass objects reaching the disk cavity will be trapped and halt migrating. The radius of the jump highly depends on the structure and the density of the disk, and it is about 0.03 AU for a disk having the same surface density

profile as the minimum mass solar nebula. This scenario correctly predicts the 2–2.5 day period censor of sub-Jupiters migrating in a tenuous disk environment. However, this scenario cannot explain the bottom edge of the sub-Jupiter desert, i.e., the presence of short-period hot super-Earths—which should also have been trapped at the disk cavity. To resolve the contradiction with observations, an appropriate modification is necessary to explain low-mass ($M < 0.02\,M_{\rm Jup}$) exoplanets on $P < 2.5$ day orbits.

This project has been supported by the Hungarian OTKA Grants K76816, K83790, and MB08C 81013, the "Lendület" Program of the Hungarian Academy of Sciences, and the "Eötvös" Fellowship of the Hungarian State.

APPENDIX

CLUSTERING WITH MAXIMAL MAHALANOBIS DISTANCE

The Mahalanobis distance of a generic vector x and the μ_1 barycenter of a given distribution, D_1, is calculated with accounting for the coordinate correlations of D_1:

$$d_M(x, D_1) = \sqrt{(x-\mu_1)^T S_{D1}^{-1}(x-\mu_1)}, \quad \text{(A1)}$$

where S_{D1} is the covariance matrix of D_1 and acts as the metric tensor in this definition. We define the Mahalanobis distance of D_1 and D_2 clusters as the sum of Mahalanobis distances of all points in D_1 from D_2, plus that of all points is D_2 from D_1:

$$d_M(D_1, D_2) = \sum_{\forall x_1 \in D_1} d_M(x_1, D_2) + \sum_{\forall x_2 \in D_2} d_M(x_2, D_1). \quad \text{(A2)}$$

The discrimination curve was defined in the mass–density space, allowing for a curvature as

$$\log(\rho) = c_1 \log(M - c_2)^{c_3}, \quad \text{(A3)}$$

where $c_{1,2,3}$ are free parameters to be fitted, ρ is the average density, and M is the mass of exoplanets. In fact, maximizing $d_M(D_1, D_2)$ does not lead to the desired result because it converges to one large cluster and another single outlier. The quantity to be optimized for is the increment of the Mahalanobis distance due to the clustering, i.e.,

$$d_M(D_1, D_2) - \langle d_M(F_1, F_2) \rangle, \quad \text{(A4)}$$

where F_1 and F_2 are disjunct clusters randomly selected from the whole sample by elements, and they have the same amount of elements as D_1 and D_2. Since there are numerical fluctuations in $d_M(F_1, F_2)$ due to the stochastical selection, Mahalanobis distances of many random clusterings must be calculated and averaged (which is represented by the $\langle\rangle$ symbols, here standing for the expectation value). Via altering $c_{1,2,3}$, the D_1–D_2 clustering varies and in such a way the discrimination in the mass–density space can be optimized for the maximal Mahanalobis distance in the period–radius space.

In our calculus, initial parameters were $c_{1,2,3} = 0.13, 0.3, 0.85$, clustering 33 objects to D_1. Mahalanobis distance was minimized with a random walk algorithm, altering the initial parameters by a factor randomly distributed normally with one expectation value and 1.5% FWHM. When the clustering converged, in total 27 exoplanets remained in the D_1 cluster.

REFERENCES

Adams, E. R., Seager, S., & Elkins-Tanton, L. 2008, ApJ, 673, 1160
Armitage, P. J. 2007, ApJ, 665, 1381
Broeg, C. 2006, PhD thesis, Univ. Jena
Broeg, C. H. 2009, Icarus, 204, 15
Chabrier, G., Baraffe, I., Leconte, J., Gallardo, J., & Barman, T. 2009, in AIP Conf. Proc. 1094, Cool Stars, Stellar Systems, and the Sun, ed. E. Stempels (Melville, NY: AIP), 102
De Maesschalck, R., Jouan-Rimbaud, D., & Massart, D. L. 2000, Chemometr. Intell. Lab. Syst., 50, 1
Douglas, L. 1976, Statistican, 25, 295
Fisher, R. A. 1925, Statistical Methods for Research Workers (Edinburgh: Oliver and Boyd)
Fortney, J. J., Marley, M. S., & Barnes, J. W. 2007, ApJ, 659, 1661
Guillot 2005, Annu. Rev. Earth Planet. Sci., 33, 493
Holman, M. J., et al. 2010, Science, 330, 51
Howard, A. H., et al. 2010, Science, 330, 653
Ida, S., & Lin, D. N. C. 2008, ApJ, 685, 584
Ivezić, Ž., et al. 2002, AJ, 124, 2943
Lecavelier des Etangs, A. 2007, A&A, 461, 1185
Mahalanobis, P. C. 1936, Proc. Natl Inst. Sci. India, 2, 49
Martin, R. G., Lubow, S. H., Pringle, J. E., & Wyatt, M. C. 2007, MNRAS, 378, 1589
Masset, F. S., Morbidelli, A., Crida, A., & Ferreira, J. 2006, ApJ, 642, 478
Mordasini, C., Alibert, Y., & Benz, W. 2009, A&A, 501, 1139
Rogers, L. A., & Seager, S. 2010, ApJ, 716, 1208
Schlaufman, K. C., Lin, D. N. C., & Ida, S. 2010, ApJ, 724, L53
Schneider 2010, Extrasolar Planet Catalog 2.03, 2010/10/21, http://exoplanet.eu/catalog.php
Valencia, D., Sasselov, D. D., & O'Connell, R. J. 2007, ApJ, 656, 545
Winn, J. 2011, in EXOPLANETS, ed. S. Seager (Tucson, AZ: Univ. Arizona Press), in press (arXiv:1001.2010)